Science of the Total Environment 633 (2018) 59–70

Contents lists available at ScienceDirect

Science of the Total Environment

journal homepage: www.elsevier.com/locate/scitotenv

Long-term trends in submicron particle concentrations in a metropolitan area of the northeastern United States

Mauro Masiol [a,b], Stefania Squizzato [a,b], David C. Chalupa [c], Mark J. Utell [c,d], David Q. Rich [a,c,d], Philip K. Hopke [a,b,*]

[a] Department of Public Health Sciences, University of Rochester Medical Center, Rochester, NY 14642, United States
[b] Center for Air Resources Engineering and Science, Clarkson University, Potsdam, NY 13699, United States
[c] Department of Medicine, University of Rochester Medical Center, Rochester, NY 14642, United States
[d] Department of Environmental Medicine, University of Rochester Medical Center, Rochester, NY 14642, United States

HIGHLIGHTS

- Long term trends in particle number concentrations have been determined.
- There were declines from 2002 to 2011 and an increase from 2011 to now.
- The decline is likely due to reductions in fuel S content and economic conditions.
- The increase may be the result of increases in the size of the light duty fleet.

GRAPHICAL ABSTRACT

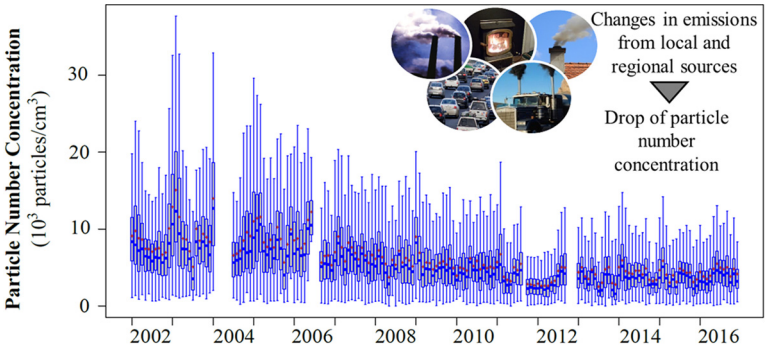

ARTICLE INFO

Article history:
Received 12 December 2017
Received in revised form 14 March 2018
Accepted 14 March 2018
Available online xxxx

Editor: P. Kassomenos

Keywords:
Ultrafine particles
Trends
Sources
Number concentration

ABSTRACT

Significant changes in emission sources have occurred in the northeastern United States over the past decade, due in part to the implementation of emissions standards, the introduction and addition of abatement technologies for road transport, changes in fuel sulfur content for road and non-road transport, as well as economic impacts of a major recession and differential fuel prices. These changes in emission scenarios likely affected the concentrations of airborne submicron particles. This study investigated the characteristics of 11–500 nm particle number concentrations and their size spectra in Rochester, NY during the past 15 years (2002 to 2016). The modal structure, diurnal, weekly and monthly patterns of particle number concentrations are analyzed. Long-term trends are quantified using seasonal-trend decomposition procedures based on "Loess", Mann-Kendall regression with Theil-Sen slope and piecewise regression. Particle concentrations underwent significant ($p < 0.05$) downward trends. An annual decrease of −323 particles/cm^3/y (−4.6%/y) was estimated for the total particle number concentration using Theil-Sen analysis. The trends were driven mainly by the decrease in particles in the 11–50 nm range (−181 particles/cm^3/y; −4.7%/y). Slope changes were investigated annually and seasonally. Piecewise regression found different slopes for different portions of the overall period with the strongest declines between 2005 and 2011/2013, followed by small upward trends between 2013 and 2016 for most size bins, possibly representing increased vehicular traffic after the recovery from the 2008 recession.

* Corresponding author at: Department of Public Health Sciences, University of Rochester Medical Center, Rochester, NY 14642, United States.
E-mail address: phopke@clarkson.edu (P.K. Hopke).

https://doi.org/10.1016/j.scitotenv.2018.03.151

1. Introduction

High concentrations of airborne particulate matter (PM) have repeatedly been associated with adverse effects upon human health (e.g., Dadvand et al., 2013; Atkinson et al., 2015; Kioumourtzoglou et al., 2016; Knibbs et al., 2011; Shi et al., 2016; Wang et al., 2017). Mass concentrations have been measured as the metric for assessing PM pollution and are regulated in many countries to protect public health. However, number concentrations also produce adverse effects on human health (Frampton et al., 2012; Rich et al., 2012, 2016; Ostro et al., 2015; Lanzinger et al., 2016), depending on their size (Valavanidis et al., 2008; Strak et al., 2012), chemical composition (Rohr and Wyzga, 2012; Atkinson et al., 2015), and the nature of sources (Kelly and Fussell, 2012; Cassee et al., 2013).

Ultrafine particles (UFPs, <100 nm) account for most of the number concentrations, but generally have negligible mass and are not well correlated with PM mass (Jeong et al., 2004). Despite extensive discussion of introducing UFPs metrics into U.S. regulatory system (e.g., Baldauf et al., 2016), particle number concentration (PNC) has not be promulgated as a National Ambient Air Quality Standard (NAAQS). UFPs can reach the deep regions of the lung (Salma et al., 2015), may translocate to other parts of the body (HEI Review Panel, 2013), and have high surface area that potentially enhances the absorption of volatile and semi-volatile species (Kelly and Fussell, 2012; Strak et al., 2012). In urban environments, UFPs are emitted by combustion, such as motor vehicle exhaust (Pant and Harrison, 2013; Kumar et al., 2014; Karjalainen et al., 2014), maritime, rail, and airport emissions (Reche et al., 2011; Masiol and Harrison, 2014; Anderson et al., 2015; Jeong et al., 2017), industrial activities and waste incineration (Riffault et al., 2015; Buonanno and Morawska, 2015), biomass burning (Chandrasekaran et al., 2013; Corsini et al., 2017) and some non-combustion sources (e.g., Kumar et al., 2013). UFPs may also form by nucleation of low volatility compounds and grow in the atmosphere (Zhang et al., 2012; Kulmala et al., 2014; George et al., 2015; Seinfeld and Pandis, 2016). Particles formed via nucleation dominate the global total particle number abundance (Yu et al., 2010). New particle formation (NPF) of regional origin is extensively reported in both rural/remote areas (e.g., O'Dowd et al., 2010; Jeong et al., 2010; Rose et al., 2015; Yu et al., 2015) and anthropogenic environments (e.g., Stanier et al., 2004; Jeong et al., 2004; Qian et al., 2007; Costabile et al., 2009; Brines et al., 2015; Salma et al., 2016; Dai et al., 2017).

Significant changes in emissions have occurred in the northeastern United States over the last several decades with reported changes in the concentration and composition of airborne particulate matter (Hogrefe et al., 2004; Frost et al., 2006; Tagaris et al., 2007; Pye et al., 2009; Dallmann and Harley, 2010; Duncan et al., 2016; Nopmongcol et al., 2016; Brown-Steiner et al., 2016). In particular, substantial decreases in the emissions of SO_2 and nitrogen oxides, two main inorganic secondary particle precursors, were recently reported for northeastern U.S. cities (Duncan et al., 2016; Emami et al., 2018).

The car fleet has changed in the U.S. after the implementation of emissions standards for on-road vehicles. Tier 2 standards for light-duty vehicles were phased in between 2004 and 2010 (US EPA, 2017). However, Tier 2 standards include light (<8500 lb gross vehicle weight rating, GVWR) and medium duty (<10,000 lb GVWR) vehicles. These changes include computerized engine control and addition of after treatment technologies. These have been continuously improved and have led to significant exhaust emission reductions (Bishop and Stedman, 2008; Bishop et al., 2012; McDonald et al., 2013; May et al., 2014).

Similarly, all new heavy-duty diesel trucks sold after July 1, 2007 must be equipped with catalytic regenerative traps (CRTs). NO_x controls are required for heavy-duty diesel vehicles sold after January 1, 2010 (US EPA, 2016a). To support the use of CRTs, the on-road diesel fuel sulfur program, as part of the 2007 Heavy-Duty Highway Rule (US EPA, 2016b), resulted in the reduction of on-road diesel fuel sulfur content in 2006/2007 from <500 ppm (low sulfur diesel fuel, LSDF) to <15 ppm (ultralow sulfur diesel, ULSD). Prior to 2007, the sulfur content of non-road diesel could be as high as 3000 ppm. From June 1, 2007 to 2014, low sulfur diesel fuel and ULSD fuel were phased in for nonroad, locomotive, and marine (NRLM) diesel fuel (US EPA, 2016b). However, in the northeastern US, nonroad diesel and locomotive fuel had to be ultralow by 2010 and 2012, respectively. After January 1, 2014, all nonroad diesel fuel in the United States was required to be ULSD. In New York State, all distillate oils sold for any purpose after July 1, 2012 (including building heating and on-road and off-road fuels) were required to be ultralow sulfur (ULS) (NYS-CRR, 2017). Furthermore, in 2008/9, coal used for power generation started to decline and natural gas increases both at national and state level, because of the changes in relative price of these fuels (EIA, 2017; New York State, 2017). In the meantime, US faced one of the worst financial/economic crisis of the last century followed by a recession period that can likely affect pollutants emissions and sources.

Emami et al. (2018) have analyzed the trends in air pollutants including gaseous pollutants, $PM_{2.5}$ and it chemical constituents in Rochester, NY.. The monthly average $PM_{2.5}$ mass showed a downward trend (-5 μg/m^3; -41%) between 2001 and 2015. This change is largely due to reductions in particulate sulfate that showed a 65% decrease. The 2001 to 2015 concentration trends were generally negative, but positive values were obtained for Delta-C (DC = black carbon measured at 370 nm – black carbon measured at 880 nm), O_3, and K^+. Elemental carbon (EC) had a trend with a positive slope from 2001 to 2004 (8.32%/y) and a negative trend (-7.18%/y) from 2005 to 2015. Extensive discussion of the influence of local and regional sources on air pollutants in Rochester is provided by Emami et al. (2018).

Ongoing measurements of submicron (11–500 nm) particle number size distributions (PNSDs) began in January 2002 in Rochester, a city representative of medium sized metropolitan areas in the northeastern United States. Prior studies of these data included analyses of particle size distributions and other air pollutants (Wang et al., 2011a, 2012), the characterization of nucleation events (Jeong et al., 2004, 2006) and source apportionment (Ogulei et al., 2007; Kasumba et al., 2009). The analysis of long-term trends of the measured particle number concentrations is also needed to determine the success of past and current mitigation strategies.

The goals of the present study were to analyze data for all 15 years (2002–2016), examining monthly, weekly, and hourly concentration patterns and to quantify their inter-annual trends. Similar analyses were performed on the criteria pollutants that were measured concurrently at the same monitoring stations in Rochester (Emami et al., 2018).

2. Materials and methods

2.1. Study area

Rochester (~210,000 inhabitants, 2010 Census) lies on the southern shore of Lake Ontario. It is the center of a metropolitan area (~1.1 million inhabitants) encompassing several counties. A map is provided as Supplementary Information Fig. S1. The local emissions scenario includes typical diffuse urban emissions and limited industrial sources. Intense vehicular traffic emissions arise from local roads and high traffic highways. Natural gas (sometime bottled LPG) is primarily used for domestic and commercial heating with a recent increase in residential wood combustion for space heating. Industrial emissions of UFPs and SO_2 were largely dominated by: (i) a 260 MW coal-fired power plant (Jeong et al., 2004, 2006; Wang et al., 2012), which was fully shut down in April 2008; and (ii) a coal-fired cogeneration plant, in which production substantially dropped during recent years. Other air pollution sources are off-road transport (diesel rail, shipping, and airport emissions), and the regional transport of polluted air masses from the Ohio River Valley, Ontario, and the eastern U.S (Emami et al., 2018).

2.2. Experimental

PNSDs were measured from January 2002 to February 2004 at a site on the roof of the main fire house surrounded by an inner loop road (~86,000 vehicles/day) within 0.5 mi of downtown Rochester (FIR: USEPA site code 36-055-6001; 43°09′40″ N, 77°36′12″ W). In May 2004, the site was moved to the current air quality monitoring site (DEC: USEPA site code 36–055-1007; 43°08′46″ N, 77°32′52″ W) in a residential environment ~300 m from the intersection of two major highways (I-490 and I-590) with an average traffic count of ~230,000 vehicles/day. The tracks of a class 1 railroad also lie adjacent to the site. A detailed map of the study area is provided in Fig. S1. Five-minute, time-resolved PNSDs (32 channels per decade) were measured using a scanning mobility particle spectrometer (SMPS) composed of a differential mobility analyzer (TSI, DMA model 3071) and a condensation particle counter (TSI, CPC model 3010). Details are reported in Jeong et al. (2004) and Kasumba et al. (2009). Anomalous and/or inconsistent records were removed, and averaging was performed to produce a dataset at a 1-hour time resolution.

2.3. Data analysis

Data analyses were performed in R (R Core Team, 2017). The long-term trends were analyzed using three different approaches applied to the monthly-averaged data. Since missing data can affect the analysis, averages were computed only for months having at least 75% of the available records. To begin, a seasonal-trend decomposition time series procedure based on 'Loess' (STL; Cleveland et al., 1990) was performed to model the shape of trends and their seasonal variations. The conceptual framework of STL is that a time series can be decomposed into three parts: seasonal, trend, and residuals. In addition, there is local regression smoothing (LOESS) so that smooth estimates are obtained for all possible time values. This technique is built into the openair R package. STL was previously used in several studies (Carslaw, 2005; Bigi and Harrison, 2010; Masiol et al., 2014). Missing data cannot be handled by STL. Thus, they were interpolated by applying a seasonal Kalman filter (Zeileis and Grothendieck, 2005). Since data are not normally distributed (Shapiro-Wilk test at $p < 0.05$), the STL analysis was performed in the robust mode. The window parameter, which sets how quickly the seasonality evolves, was chosen after applying values from 3 to 21 (increasingly constant seasonality) and "periodic" (no changes in seasonality). A value of seven was chosen as the best compromise accounting for variations due to the relatively fast changes in emission scenarios (sometime within 1 year). Confidence intervals (95%) for trends and seasonality were then generated by bootstrapping ($n = 5000$).

In a second step, the linear trends were computed through the Mann-Kendall trend analysis (Mann, 1945; Kendall, 1975) and the Theil-Sen nonparametric estimator of slope (Theil, 1950; Sen, 1968). This technique assumes monotonic linear trends and therefore, is useful in estimating the interannual trends. However, it does not take the shape of trends into account, e.g., it does not consider possible breakpoints. Since the emissions scenario in Rochester underwent multiple changes, the monthly-averaged particle number concentrations were also investigated for the detection of segmented trends with different slopes using piecewise regression analysis. For this purpose, the most plausible locations of breakpoints were estimated using the "segmented" package (Muggeo, 2003, 2008). It uses an interactive procedure that requires approximate starting values for the breakpoints and implements bootstrap restarting (Wood, 2001) to estimate both slopes and breakpoint positions with standard errors.

3. Results and discussion

The averaged total PNC (all data, 2002 to 2016) was 5.9×10^3 particles/cm^3 (Fig. S2). This concentration was generally lower than those values reported for other major cities of NE US: e.g., New York City, 8.2×10^3 particles/cm^3 (Masiol et al., 2017a, 2017b); Toronto, 8×10^3 particles/cm^3 (Jeong et al., 2010) in spite of these other cities using measurement systems with lower cutoff diameters >11 nm.). PNSDs were split into three ranges roughly representative of nucleation (11–50 nm; PNC 11–50), Aitken nuclei (50–100 nm; PNC 50–100) and accumulation mode (100–500 nm; PNC 100–500) particles. On average, the mean concentrations in these three ranges were 3.5×10^3, 1.5×10^3, and 0.9×10^3 particles/cm^3, respectively (Fig. S2).

The data were separated both seasonally and by 3-year periods. Changes in emission sources, actinic fluxes and resulting photochemistry, and meteorology drive strong seasonal variations in the particle sizes. Three seasons were defined as done in previous studies (e.g., Kasumba et al., 2009): summer (Jun-Jul-Aug), winter (Dec-Jan-Feb) and transition (6 remaining months). Five 3-year periods were selected to investigate the possible changes in size spectra over the total period. The 2002/2004 period includes data collected at FIR, while remaining periods (2005/2007 through 2014/2016) from east side site (DEC).

Analysis of the data showed non-normal distributions for the variables. Thus, the nonparametric Kruskal-Wallis analysis of variance on

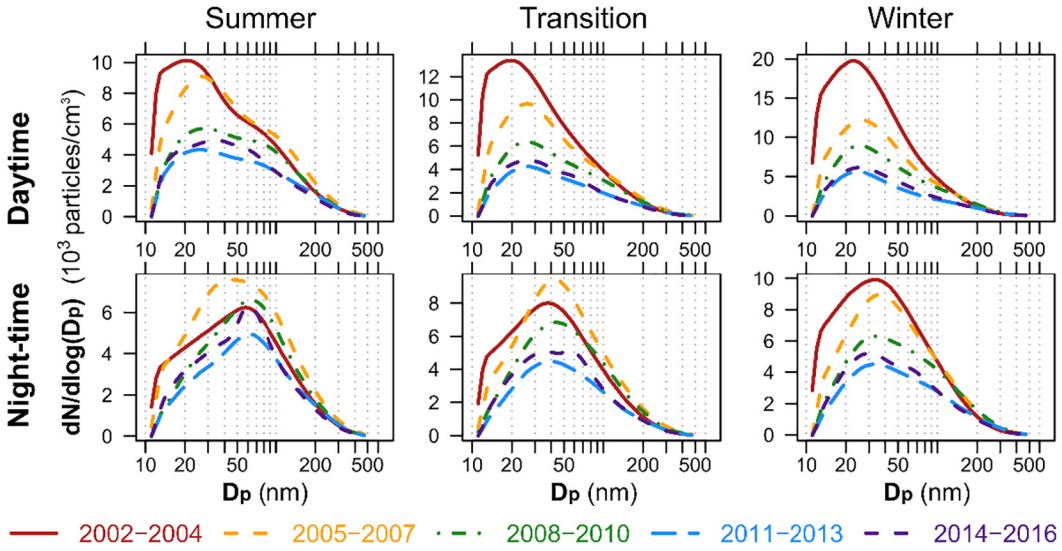

Fig. 1. Average size distributions for PNSDs recorded during the 5 sampling periods and categorized by season and daytime/nighttime. Detailed statistics of the size distributions for particle number and volume concentrations are provided separately in Figs. S2 and S3.

ranks was used to test the difference in concentration between summer and winter (all data 2002/16). Concentrations of total PNC (TPNC), PNC 11–50 and PNC 100–500 (Table S1) were different at the $p = 0.05$ significance level, while PNC 50–100 concentrations were similar ($p = 0.18$). This result is an indication of the seasonal effect on the size distributions. Higher average total PNC concentrations were recorded in the winter (6.5×10^3 particles/cm^3; Fig. S2), while summer and transition periods exhibited similar concentrations (~5.7×10^3 particles/cm^3). The higher concentrations in the winter were largely driven by PNC 11–50 (average 4.1×10^3 particles/cm^3), while PNC 50–100 and PNC 100–500 particles were similar to the summer and transition periods. Despite having similar average total PNC concentrations (Table S1), summer had lower average concentrations of PNC 11–50 (2.9×10^3 particles/cm^3), but higher concentrations of PNC 50–100 and PNC 100–500 relative to the other seasons (Fig. S2).

The PNSDs and particle volume size distributions (PVSDs) categorized by time of day (7 am–7 pm and 7 pm–7 am local time), season, and by each of the five 3-year periods are presented in Fig. S3 (daytime) and Fig. S4 (nighttime). A summary of the average PNSDs concentrations is provided in Fig. 1. The day/night split permits study of the changes in the size spectra due to the actinic flux and resulting photochemistry, anthropogenic activities such as traffic and building heating, and meteorology (e.g., mixing layer dynamics, air temperature). Results for the summer (Figs. 1 and S3) show that the average daytime PNSD is dominated by a large nucleation range mode and a second mode in the Aitken range. A relatively constant decline in the nucleation mode occurred over the 5 periods, while the Aitken mode was almost constant in number, but the geometric standard deviation became smaller (Fig. 1). The main changes in the structure of the nucleation mode occurred between 2002 and 2004 and 2005–2007. However, this result may have been caused by the different strengths of local sources between FIR and DEC sites. In winter, despite the strong decrease in the concentrations observed over all the size bins, the daytime modal structures remained almost unchanged. The PNSDs during the transition periods showed intermediate changes between summer and winter.

All the nocturnal spectra show fewer nucleation events with respect to the daytime spectra and generally have increased concentrations of coarser particles (Fig. S4). The nocturnal PNSDs exhibited peaks around 40–60 nm in summer and transition periods. The winter nocturnal spectra are similar to the daytime ones, with a finer mode around 20–40 nm. In summary, all seasons showed decreased smallest modes during the night, while the second mode was relatively constant throughout the day. Because of the exponential relationship between particle number and volume concentrations, the modal structures of PNVDs were almost constant.

3.1. Monthly, weekly, and daily cycles

The monthly cycles of the PNC for each size range are shown in Fig. S5. The monthly average PNSD pattern (all data 2002/16) is shown as a contour plot in Fig. 2a, while the detailed monthly average patterns of PNSDs over the five 3-year periods are supplied in Fig. S6. Generally, PNC 11–50 exhibited a clear seasonal pattern with the highest concentrations in winter and lowest in the summer. The minima concentrations were commonly recorded between May and July, except for 2005–2007 and 2011–2013 (late summer-autumn). PNC 100–500 particles showed marked seasonal patterns with two maxima peaking in the warmer (May–Aug) and colder (Dec–Feb) months. The monthly cycles of 50–100 nm particles were characterized by patterns similar to the accumulation mode particles. The contour plots of the monthly averages for PNSDs during the five 3-year periods (Fig. S6) show: (i) a general decrease in concentrations for UFPs from 2002/2004 to 2014/2016; (ii) the highest concentrations for particles in the 11–50 nm range were between January and March. The contour plot also shows a drop of concentrations for particles below 50 nm during the summer (more evident around July) that is likely related to the higher mixed layer heights and higher ventilation coefficients in summer.

The diel cycles over a week for each of the three size ranges are shown in Fig. 3. The diel patterns of PNSD (computed for all data 2002/16) is shown as a contour plot in Fig. 2b, while the detailed monthly average patterns of PNSDs over the five multiyear periods are presented in Fig. S7. The hourly traffic counts for the NY590 (approx. 2.5 km NNE to the DEC site; Fig. S1) were obtained from the NYS Dept. of Transportation (DoT) for the 2010/2015 period. The time patterns are presented in Fig. S8. Similar weekly and hourly patterns were found for PNC 11–50 and PNC 50–100 over all the sampling periods (Fig. 3). The timing and the extension of peaks in the summer and winter were often different with the transition period patterns having a mixed behavior. PNC 11–50 exhibit 3 peak concentration values related to nucleation events (Jeong et al., 2004):

- Morning concentration maxima occurring during rush hours (7–8 am local time) during all seasons, but are mostly evident in winter (all data seasonal average ~6×10^3 particles/cm^3) and weaker in summer;
- Early afternoon concentration peaks occurring around noon in the summer and in the early afternoon in the winter (2–4 pm), and are generally related to photochemically driven NPF; and
- Evening concentration maxima mostly occurring in the late evening in summer (9–11 pm) and in the late afternoon in winter (4–6 pm).

While the winter evening, concentration maxima were concurrent with the evening rush hours (Fig. S8), the summer evening peaks were more likely related to mixing layer dynamics. PNC 50–100 show deep minima around noon and 2 main peaks: (i) similar to PNC 11–50, morning maxima during rush hour (7–8 am local time) during all seasons but most evident in winter (all data seasonal average ~ 1.6×10^3 particles/cm^3); and (ii) evening maxima occurring in the late evening in summer (9–11 pm) and evening in winter (7–9 pm). The transition season patterns and winter are comparable for PNC 50–100. However, the patterns during summer are highly variable.

The weekly-hourly pattern of size spectra (Fig. 2b) shows the different modal structures of the three main peaks occurring during weekdays. While the morning peak extends over a wide size range (12–100 nm), the evening peak involves larger particles (20 to 100 nm). The peak around noon included particles in the smaller size range (peaking at 20–30 nm) and generally experienced growth until the evening peak. During the weekends (mostly Sundays), the morning peak disappears (limited road traffic), while the other two peaks remained (but had lower intensity).

3.2. Seasonal variations

The variation of monthly average concentrations in each of the three size modes are shown in Fig. 4 and presented in Table S1. The number concentrations of the nuclei and Aitken mode particles have a peak in the winter during the early years. Winter maxima result from the lower temperatures enhancing the nucleation of combustion emissions particularly from motor vehicles, and lower mixed layer heights and wind speeds. However, accumulation mode particle concentrations peak in the summer when higher photochemical activity produces more secondary species including those particles transported into the region. Over the time of these measurements, the seasonal differences become smaller and smaller as the number concentrations also decreased. Sabaliauskas et al. (2012) reported number concentrations for the same three modes measured in Toronto from 2006 to 2011. They reported substantially higher concentrations and larger seasonal differences than were observed in Rochester during this period. Their measurement site is closer to a major roadway and Toronto has a significantly larger population than Rochester.

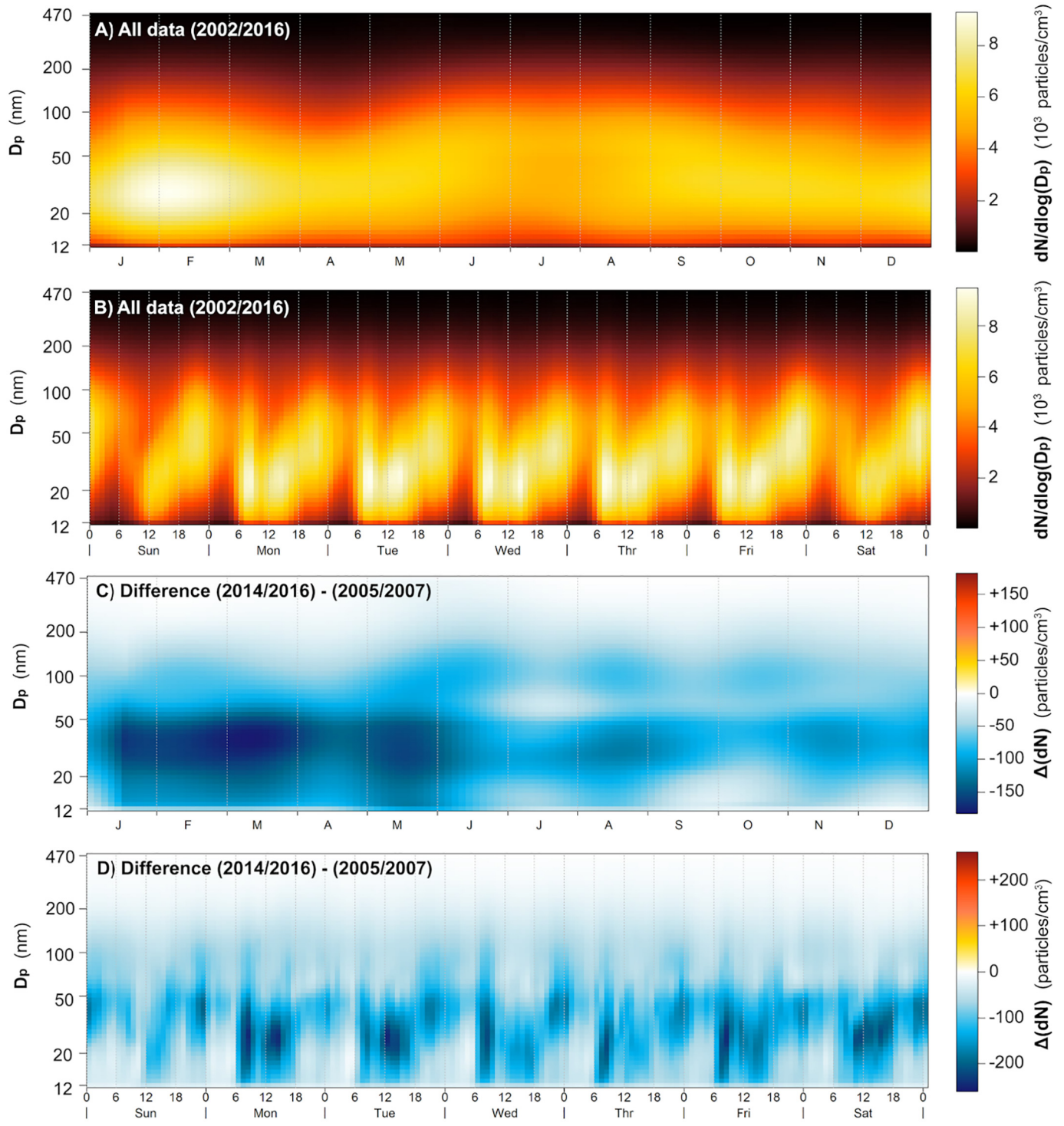

Fig. 2. Monthly (a) and weekly-hourly (b) average patterns of PNSDs calculated over all the data. Monthly (c) and weekly-hourly (d) differences between the average concentrations measured during the 1st period (2005–2007) and the last period (2014–2016) at the site DEC.

3.3. Trend analyses

Since the SMPS data were collected at 2 sites (FIR and DEC) with different characteristics (e.g., different orientation with respect to the industrial source emissions and main highways), the trend analyses were only computed for data collected at DEC. A separate trend analysis over the data collected at FIR is impossible due to the short time series (<2 years of available data). In addition, since the variables are affected by strong seasonality, it is advisable to include full years in calculations: the first data collected at east side DEC site (July 2004–December 2004) were removed from the trend computations. In summary, trends were computed over 12 years (2005/2016).

Fig. 5 summarizes the results of the trend analyses over the total PNC and the three size ranges. Tables 1 and 2 report the results of Theil-Sen analyses and piecewise regressions, respectively. Fig. 6 shows the contour plot of the STL results for the monthly-averaged PNSDs as well as the results of the differential STL, i.e. the concentration of each size bin i during the month j (j in Jan 2005–Dec 2016) were obtained by

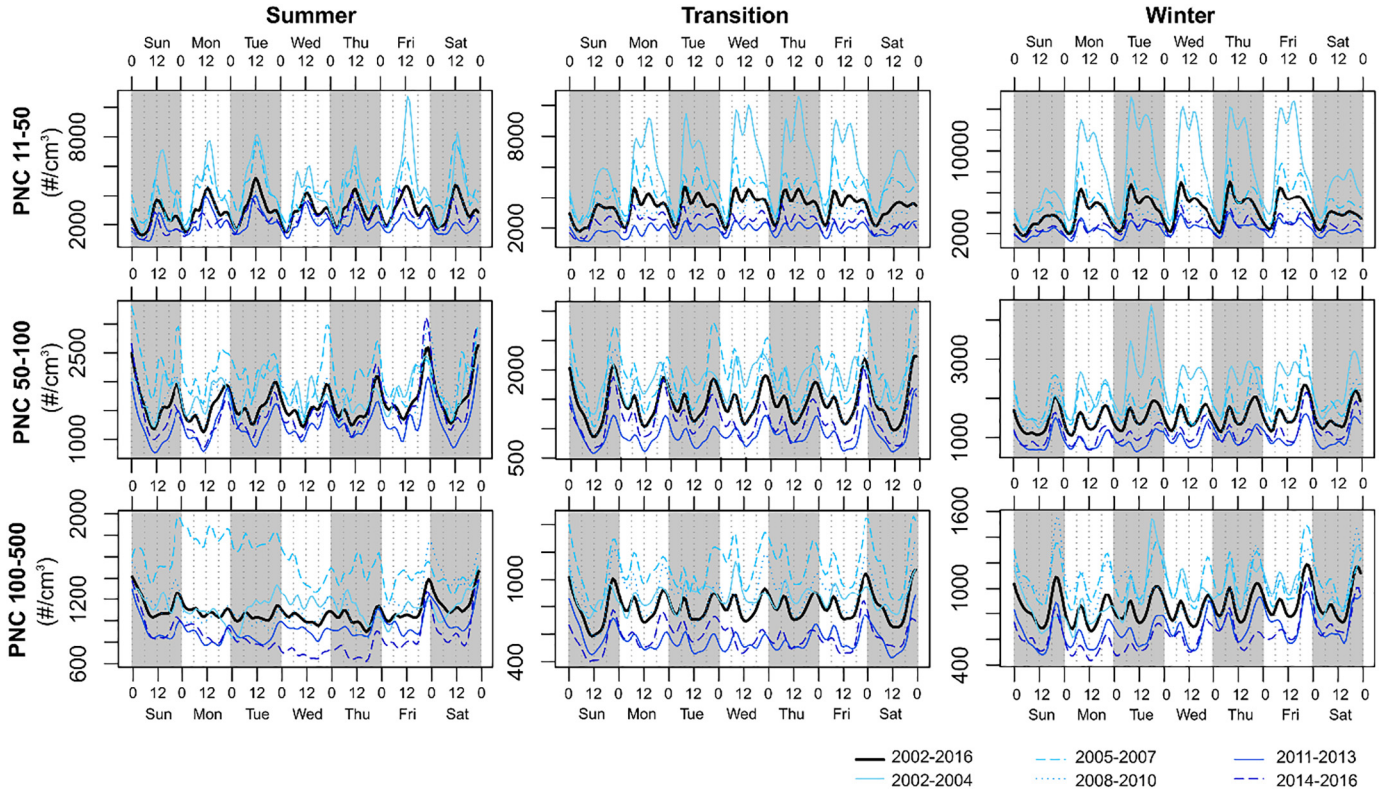

Fig. 3. Average week-hourly cycles of the 3 particle ranges (nucleation 12–50 nm; Aitken 50–100 nm; accumulation 100–500 nm) measured over the 5 selected periods and the 3 seasons. The black solid line represents the average patterns of all the data (2002–2016).

subtracting the concentration modeled by the STL of bin *i* at the month *j*-1. The STL analysis shows a rapid decrease in the concentrations of PNC 11–50, PNC 50–100, and consequently, total PNC during 2005/2008. The STL and differential STL over all the size spectra show that this strong drop mostly resulted from particles in the 18–80 nm range between 2005 and 2006. This decline could be in part due to decreased emissions from the 260 MW coal-fired power plant that closed in early 2008 and the reductions in on-road diesel fuel sulfur as suggested by Wang et al. (2011a, 2011b).

PNC 11–50, PNC 50–100, and consequently, total PNC exhibited a decline (approx. 1 year-long) in concentrations during the 2nd half of 2011 with subsequent concentration increases in the first half of 2012 (Fig. 5). This anomaly is clearly observed in the STL and the differential STL analyses for the PNSDs (Fig. 6). Scrutiny of the raw data excluded any instrumental issues. There were no evident changes in meteorology, including average wind speed, and amount of precipitation. There are no known changes in emissions for this period. Thus, the reasons driving this decrease in concentration remains unclear. This period was included in the subsequent Theil-Sen trend analysis, but it was excluded from the piecewise regression (October 2011 to June 2012). The differential STL analysis also exhibits a slight but detectable (according to the STL 95% confident interval) increase in the number concentration of particles smaller than ~80 nm (peaking at approx. 20–70 nm) in 2015–2016. This trend is also detected for PNC 50–100 and PNC 11–50 (Fig. 5).

The median linear Theil-Sen slopes computed over all the seasons (annual) show highly statistically significant ($p < 0.001$) downward trends for all the size ranges and total PNC (Table 1). A median linear drop of −323 particles/cm^3/y (−4.6%/y) was estimated for the total PNC (Fig. 5). The trends were mainly driven by the decrease of particles in the 11–50 nm range (−181 particles/cm^3/y; −4.7%/y). PNC 50–100 dropped by −84 particles/cm^3/y (−4.2%/y) while PNC 100–500 declined by −53 particles/cm^3/y (−4.5%/y). The percent trend values are comparable to those reported for other air pollutants in Rochester during 2005/2015 (Emami et al., 2018), including CO (−7.9%/y), $PM_{2.5}$ (−3.7%/y), and $PM_{2.5}$-bound species such as nitrate (−4.8%/y), sulfate (−7.1%/y), organic and elemental carbon (−3.1 and − 7.1%/y, respectively) and black carbon (−5.5%/y). However, the trend was lower than that reported for SO_2 (−10.2%/y), a major secondary particle precursor. Thus, submicron particle concentrations underwent similar trends as observed for most of the analyzed air pollutants in Rochester. This result suggests that recent and past mitigation strategies for air pollution in U.S. and generally, in North America, have resulted in improved air quality.

Theil-Sen slopes were estimated for each PNSD size bin (Fig. 7). The results (upper-left plot) show that all slopes were statistically significant ($p < 0.001$) with median slopes between −6 and − 4%/y. However, sharper downward slopes were generally observed for the two smallest sizes (<13 nm) and particles in the 30–50 nm range (Table 1).

Piecewise linear regressions (Table 2; Fig. 5) showed the best fits with one breakpoint, except for PNC 100–500, whose decrease was better estimated with no breakpoints. However, the adjusted coefficients of determination were high ($r^2 > 0.6$) only for PNC 11–50 and total PNC. The faster drop of PNC 11–50 (−595 particles/cm^3/y) occurred between January 2005 and summer 2009. This pattern reflects both the effects of mitigation policies in NYS and Rochester, e.g., the use of ultralow sulfur fuels (2006/2008), the shutdown of the large coal-fired power plant (Fig. S1) completed in April 2008 (Wang et al., 2011b), and the economic recession of 2007 to 2009. The subsequent decrease in concentrations was lower (−52 particles/cm^3/y). PNC 50–100 showed a downward trend (−121 particle/cm^3/y) before the summer of 2013 and a subsequent increase in concentration (+58 particles/cm^3/y). The piecewise regression of PNC 100–500 showed a constant drop of −58 particles/cm^3/y, but a poor fit (r^2~0.4) largely due to monthly variations. This result was found even with the selection of only one breakpoint.

Trend analyses were repeated for each of the 3 seasons. Results are given in Tables 1 and 2, and Figs. 5 and 7. Theil-Sen slopes were still

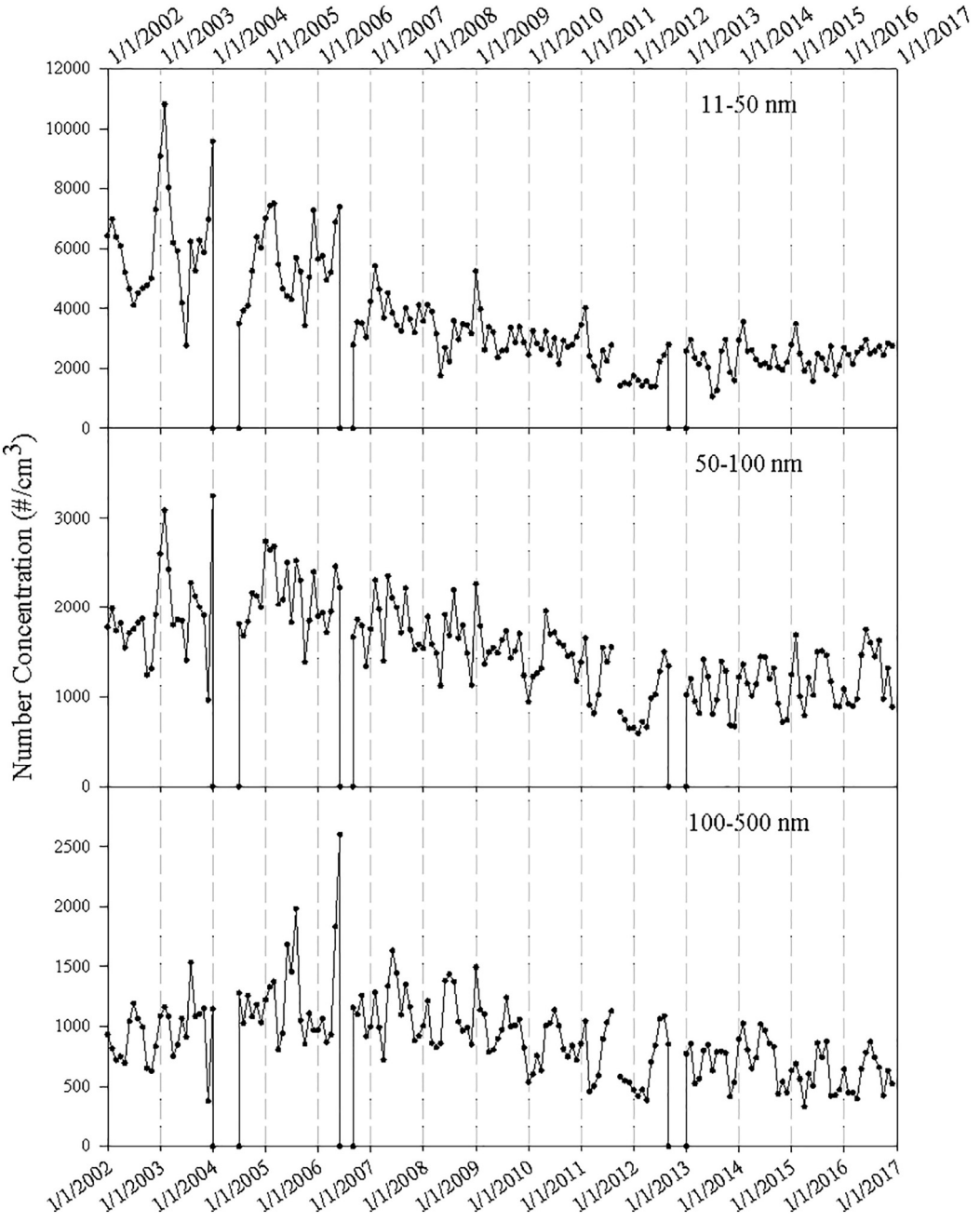

Fig. 4. Plot of monthly average number concentrations (#/cm^3) for each of the three size bins.

statistically significant ($p < 0.01$) for each season, and all slopes were negative. Generally, the negative Theil-Sen slopes were larger in the winter (total PNC: −394 particles/cm^3/y) than in the summer (total PNC: −241 particles/cm^3/y). The Theil-Sen slope estimated for each size PNSD bin (Fig. 7) indicated that slopes were similar to those calculated for the whole year. Spectra for the summer and transition periods exhibited similar profiles to the annual one, while the slope spectrum for winter exhibited more rapid decreases in the smallest size particles and statistically insignificant slopes ($p > 0.05$) for the coarsest particles (>300 nm).

Piecewise linear regression (Fig. 8) showed that one breakpoint was sufficient to obtain good fits for most sizes and seasons, with r^2 values generally higher than those obtained for the annual data. However, PNC 100–500 were still poorly modeled with no breakpoints in summer and winter due to their high variance. In summer, higher linear negative trends were recorded until summer 2013. For transition and winter seasons, the breakpoints occurred between spring 2011 and winter 2011/2012, i.e. during the concentrations dip found by the differential STL analysis (Fig. 6). This result is stable regardless of the inclusion or exclusion of the data between October 2011 and June 2012, i.e. clear changes of slope occurred in this period. All the linear regression results computed after the breakpoints indicated upward trends. This result shows a continuing increase in the concentrations of the smallest sized particles. This increase may be related to the increasing number of cars registered in Monroe County, the county in which Rochester is located (Fig. S9).

3.4. Changes in the monthly and hour of the week particle size spectra

Since trend analyses indicated extensive changes in concentrations occurred over the last 12 years, the changes in the monthly and hour of the week patterns were investigated. The differences in monthly

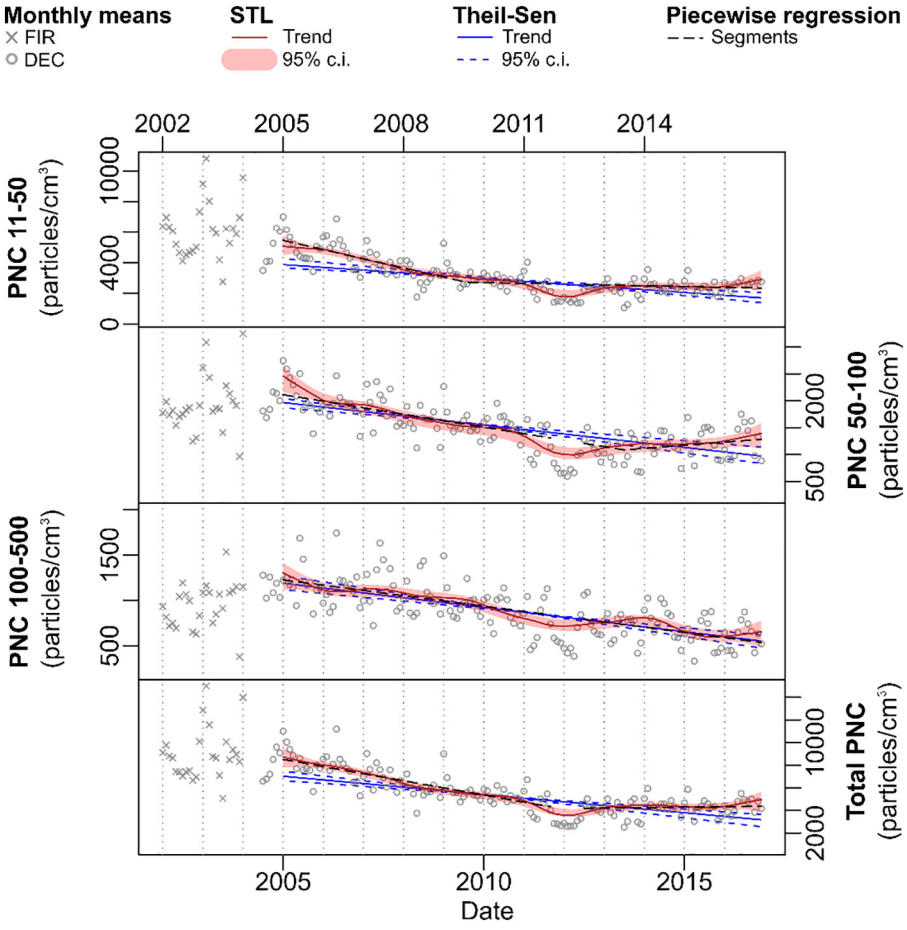

Fig. 5. Results of trend analyses (STL in red; Theil-Sen nonparametric estimator of slope in blue; piecewise linear regression model with breakpoints estimation in black). Monthly averaged concentrations of periods not included in the trend analyses are also showed. The confidence intervals (c.i. at 0.05 level) for STL and Theil-Sen slopes are computed by bootstrap estimation. (For interpretation of the references to colour in this figure legend, the reader is referred to the web version of this article.)

averages and hour of the week averages for all sizes from 2005 to 2007 and 2014–2016 are shown in Fig. 2c and d, respectively. These plots show the differences computed for each of the 5-multiyear periods (Figs. S10 and S11). The modal structure of PNSDs exhibited strong differences between 2002 and 2003 and 2005–2007 for both monthly and hour of the week results. Although these concentration changes may have been affected in part by the change in sampling sites (FIR to

Table 1
Results of the Theil-Sen nonparametric estimator of slope with Mann-Kendall tests for all data (annual) and seasons.

Period		Slope	95% c.i. range[d]	Slope	*p*
		Particles/cm³/y	Particles/cm³/y	%	
Annual	PNC 11–50	−181	−239, −134	−4.7	<0.001
	PNC 50–100	−83	−101, −61	−4.2	<0.001
	PNC 100–500	−53	−67, −42	−4.5	<0.001
	Total PNC	−323	−411, −249	−4.6	<0.001
Summer[a]	PNC 11–50	−118	−256, −23	−3.7	<0.01
	PNC 50–100	−57	−116, −31	−3	<0.01
	PNC 100–500	−68	−89, −44	−4.8	<0.001
	Total PNC	−241	−433, −104	−3.7	<0.001
Transition[b]	PNC 11–50	−185	−270, −123	−4.9	<0.001
	PNC 50–100	−82	−110, −57	−4.4	<0.001
	PNC 100–500	−52	−68, −38	−4.7	<0.001
	Total PNC	−325	−454, −239	−4.8	<0.001
Winter[c]	PNC 11–50	−232	−370, −122	−5.2	<0.001
	PNC 50–100	−97	−147, −60	−5.3	<0.01
	PNC 100–500	−56	−72, −39	−4.7	<0.001
	Total PNC	−394	−574, −240	−5.2	<0.001

[a] Summer (Jun–Jul_Aug).
[b] Transition (Mar-Apr-May-Sep-Oct-Nov).
[c] Winter (Dec-Jan-Feb).
[d] 95% confidence intervals (c.i.) computed by bootstrapping the data.

Table 2
Results of the piecewise linear regression for all data (annual) and seasons.

Piecewise regression		Breakpoints		Slope[f]	Adj. R^2
		No.[d]	Period[e]	Particles/cm³/y	
Annual	PNC 11–50	1	Jul 2009	−595, −52	0.61
	PNC 50–100	1	Jul 2013	−121, 58	0.52
	PNC 100–500	0[g]	–	−57.9	0.44
	Total PNC	1	Nov 2011	−628, 40	0.64
Summer[a]	PNC 11–50	1	Aug 2013	−295, 386	0.73
	PNC 50–100	1	Aug 2013	−132, 168	0.72
	PNC 100–500	0[g]	–	−70	0.68
	Total PNC	1	Jul 2013	−520, 531	0.78
Transition[b]	PNC 11–50	1	Nov 2011	−477, 149	0.68
	PNC 50–100	1	Apr 2012	−165, 57	0.57
	PNC 100–500	1	Nov 2011	−86, −16	0.51
	Total PNC	1	Jan 2012	−720, 206	0.68
Winter[c]	PNC 11–50	1	Jan 2012	−522, 119	0.66
	PNC 50–100	1	Feb 2012	−189, 28	0.57
	PNC 100–500	0[g]	–	−58.104	0.51
	Total PNC	1	Feb 2012	−778, 111	0.63

[a] Summer (Jun-Jul-Aug).
[b] Transition (Mar-Apr-May-Sep-Oct-Nov).
[c] Winter (Dec-Jan-Feb).
[d] Number of breakpoints included.
[e] Timing of the breakpoints (approximation to months).
[f] Slope of each segment.
[g] No breakpoints detected, thus a simple linear regression overall the data was computed.

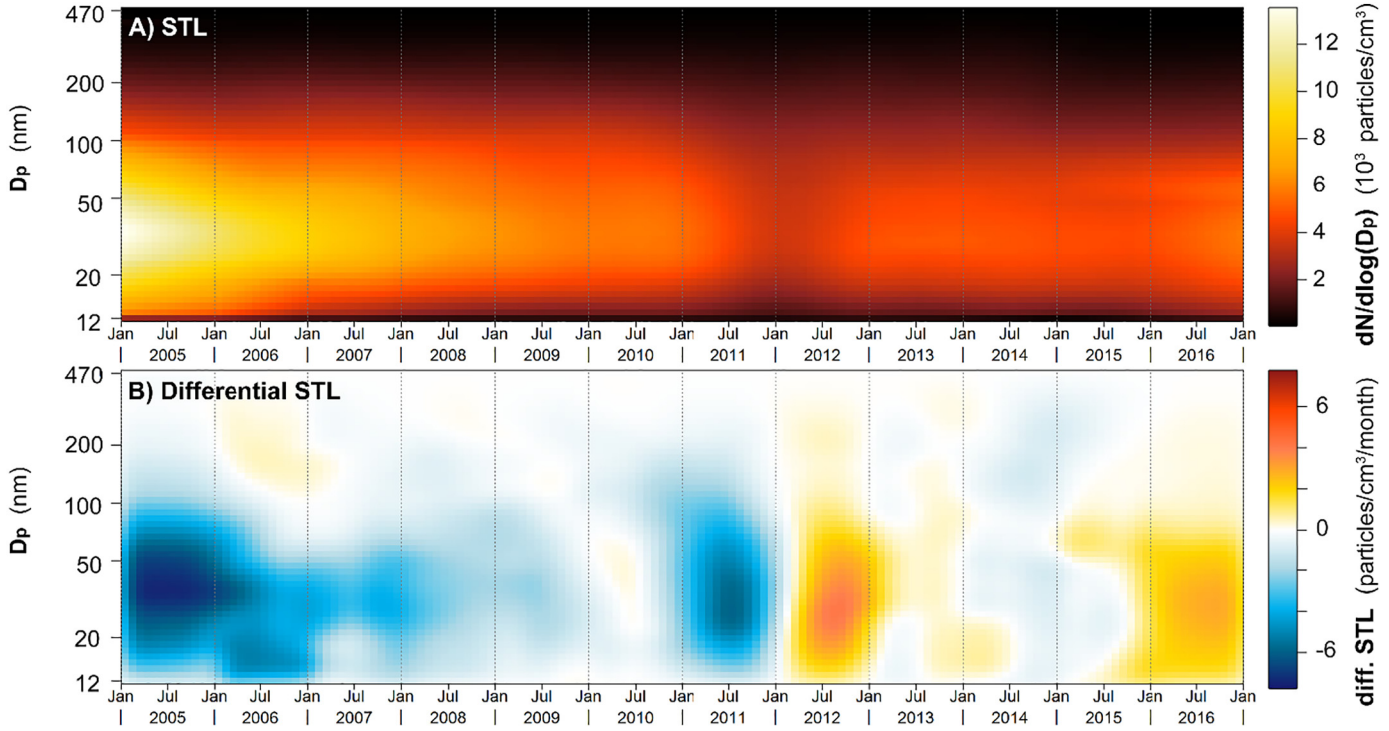

Fig. 6. Results of STL on PNSDs (upper) and differential STL (bottom).

DEC), the fastest concentration declines consistently occurred for particles below 50 nm during the coldest months (December to March) and during the day (6 am to 6 pm). The period of 2006 to early 2007 corresponds to the switch of on-road diesel fuel to ultra-low sulfur content. There were moderate concentration increases of 30–200 nm particles between May and August and during the night. This period was one of increasing economic activity following the 2002 economic recession. There were also increasing summer temperatures that increased the demand for electricity to provide air conditioning.

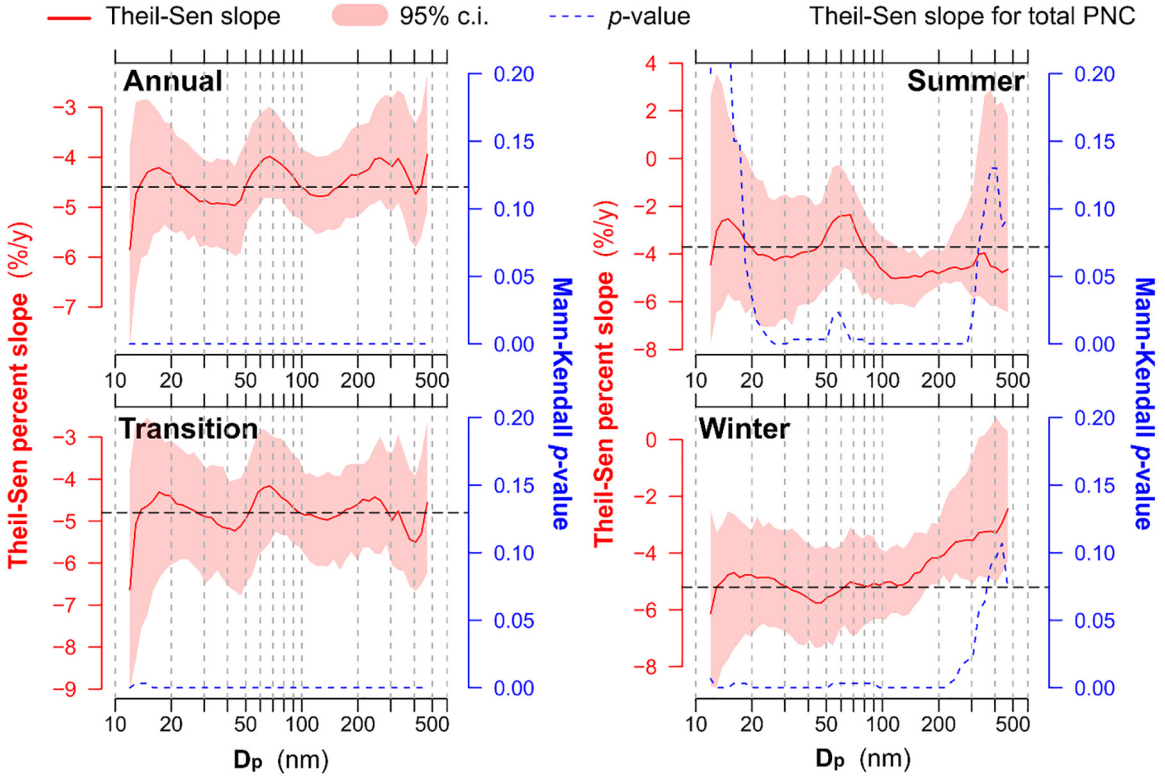

Fig. 7. Results of the Theil-Sen nonparametric estimator of slope for each SMPS bin. The confidence intervals (c.i. at 0.05 level) are computed by bootstrap estimation. The *p*-values of Mann-Kendall tests are also plotted.

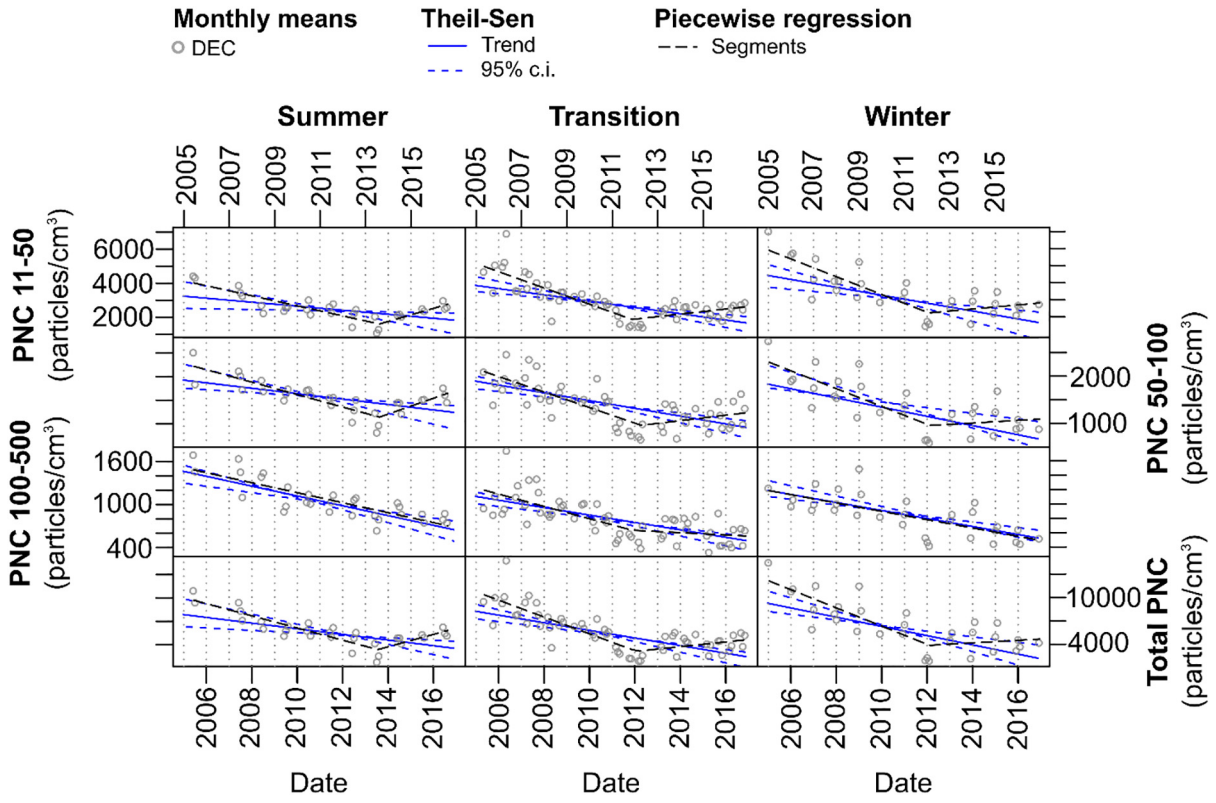

Fig. 8. Results of trend analyses (Theil-Sen nonparametric estimator of slope; piecewise linear regression model with breakpoints estimation) over the 3 seasons.

The differences in the monthly and hour of the week profiles among data collected after 2005 at the DEC site (Figs. 2c;d) show a general drop in the concentrations of particles below 50 nm during January, February, March, and May during daylight hours. It is not clear why April is anomalous. The sharpest drops coincided with the morning, midday, and evening concentration peaks (Fig. 3). This result suggests that the decreases were due to changes in the local emissions. The morning and evening peaks were related to road traffic. The midday events were generally related to photochemical transformation of locally emitted SO_2 (plume events, Jeong et al., 2004). Despite the overall drop in concentration that occurred between 2005/2007 and 2014/2016 (Fig. 2c;d), Figs. S10 and S11 show a moderate concentration increase from 2011/13 to 2014/16, especially during the morning and evening rush hours. This result is consistent with the trend analysis and may be linked to increasing road traffic emissions arising from increasing economic activity and increasing registered vehicles on the roads.

4. Conclusions

There have been substantial changes in the particle number concentrations measured in Rochester, particularly in the smallest particle size range (nucleation) mode. The initial decline in concentrations appears to follow some of the changes in fuel S content and implementation of controls on emissions from on-road heavy-duty diesel vehicles. The trends are also consistent with substantial influences from the economic recession of 2007–2009 and shift in fuels used for electricity generation resulting from the low price of natural gas. Thus, concentrations appear to have responded to both policy initiatives and the influence of economic drivers of emissions. It is likely that similar trends could be expected to have occurred in the series of moderate sized cities in the northeastern US from Buffalo, NY to Portland, ME. However, no other measurements have been made that would permit the assessment of such changes.

Acknowledgments

This work was supported by the New York State Energy Research and Development Authority (NYSERDA) under agreement #59802. The authors gratefully acknowledge the New York State Department of Environmental Conservation for their help in hosting and maintaining the SMPS operational at FIR and DEC sites in Rochester. NYS Department of Transportation provided road traffic profiles.

Appendix A. Supplementary data

Supplementary data to this article can be found online at https://doi.org/10.1016/j.scitotenv.2018.03.151.

References

Anderson, M., Salo, K., Hallquist, Å.M., Fridell, E., 2015. Characterization of particles from a marine engine operating at low loads. Atmos. Environ. 101, 65–71.
Atkinson, R.W., Mills, I.C., Walton, H.A., Anderson, H.R., 2015. Fine particle components and health—a systematic review and meta-analysis of epidemiological time series studies of daily mortality and hospital admissions. J. Expo. Sci. Environ. Epidemiol. 2563, 208–214.
Baldauf, R.W., Devlin, R.B., Gehr, P., Giannelli, R., Hassett-Sipple, B., Jung, H., Martini, G., McDonald, J., Sacks, J.D., Walker, K., 2016. Ultrafine particle metrics and research considerations: review of the 2015 UFP workshop. Int. J. Environ. Res. Public Health 13, 1054.
Bigi, A., Harrison, R.M., 2010. Analysis of the air pollution climate at a central urban background site. Atmos. Environ. 44, 2004–2012.
Bishop, G.A., Stedman, D.H., 2008. A decade of on-road emissions measurements. Environ. Sci. Technol. 42, 1651–1656.
Bishop, G.A., Schuchmann, B.G., Stedman, D.H., Lawson, D.R., 2012. Emission changes resulting from the san Pedro bay, California ports truck retirement program. Environ. Sci. Technol. 46, 551–558.
Brines, M., Dall'Osto, M., Beddows, D.C.S., Harrison, R.M., Gómez-Moreno, F., Núñez, L., Artíñano, B., Costabile, F., Gobbi, G.P., Salimi, F., Morawska, L., Sioutas, C., Querol, X., 2015. Traffic and nucleation events as main sources of ultrafine particles in high-insolation developed world cities. Atmos. Chem. Phys. 15 (10), 5929–5945.
Brown-Steiner, B., Hess, P., Chen, J., Donaghy, K., 2016. Black carbon emissions from trucks and trains in the Midwestern and Northeastern United States from 1977 to 2007. Atmos. Environ. 129, 155–166.

Buonanno, G., Morawska, L., 2015. Ultrafine particle emission of waste incinerators and comparison to the exposure of urban citizens. Waste Manag. 37, 75–81.
Carslaw, D.C.C., 2005. On the changing seasonal cycles and trends of ozone at Mace Head, Ireland. Atmos. Chem. Phys. 5 (12), 3441–3450.
Cassee, F.R., Héroux, M.-E., Gerlofs-Nijland, M.E., Kelly, F.J., 2013. Particulate matter beyond mass: recent health evidence on the role of fractions, chemical constituents and sources of emission. Inhal. Toxicol. 25, 802–812.
Chandrasekaran, S.R., Hopke, P.K., Newtown, M., Hurlbut, A., 2013. Residential-scale biomass boiler emissions and efficiency characterization for several fuels. Energy Fuel 27, 4840–4849.
Cleveland, R.B., Cleveland, W.S., McRae, J.E., Terpenning, I., 1990. STL: a seasonal-trend decomposition procedure based on loess. J. Off. Stat. 6 (1):3–73. https://doi.org/citeulike-article-id:1435502.
Corsini, E., Vecchi, R., Marabini, L., Fermo, P., Becagli, S., Bernardoni, V., Marinovich, M., 2017. The chemical composition of ultrafine particles and associated biological effects at an alpine town impacted by wood burning. Sci. Total Environ. 587–588:223–231. https://doi.org/10.1016/j.scitotenv.2017.02.125.
Costabile, F., Birmili, W., Klose, S., Tuch, T., Wehner, B., Wiedensohler, A., Franck, U., König, K., Sonntag, A., 2009. Spatio-temporal variability and principal components of the particle number size distribution in an urban atmosphere. Atmos. Chem. Phys. 9 (9):3163–3195. https://doi.org/10.5194/acp-9-3163-2009.
Dadvand, P., Parker, J., Bell, M.L., Bonzini, M., Brauer, M., Darrow, L.A., Gehring, U., Glinianaia, S.V., Gouveia, N., Ha, E., Leem, J.H., van den Hooven, E.H., Jalaludin, B., Jesdale, B.M., Lepeule, J., Morello-Frosch, R., Morgan, G.G., Pesatori, A.C., Pierik, F.H., Pless-Mulloli, T., Rich, D.Q., Sathyanarayana, S., Seo, J., Slama, R., Strickland, M., Tamburic, L., Wartenberg, D., Nieuwenhuijsen, M.J., Woodruff, T.J., 2013. Maternal exposure to particulate air pollution and term birth weight: a multi-country evaluation of effect and heterogeneity. Environ. Health Perspect. 121 (3):367–373. https://doi.org/10.1289/ehp.1205575.
Dai, L., Wang, H., Zhou, L., An, J., Tang, L., Lu, C., Yan, W., Liu, R., Kong, S., Chen, M., Lee, S., Yu, H., 2017. Regional and local new particle formation events observed in the Yangtze River Delta region, China. J. Geophys. Res.-Atmos. 122 (4):2389–2402. https://doi.org/10.1002/2016JD026030.
Dallmann, T.R., Harley, R.A., 2010. Evaluation of mobile source emission trends in the United States. J. Geophys. Res.-Atmos. 115 (14):1–12. https://doi.org/10.1029/2010JD013862.
Duncan, B.N., Lamsal, L.N., Thompson, A.M., Yoshida, Y., Lu, Z., Streets, D.G., Hurwitz, M.M., Pickering, K.E., 2016. A space-based, high-resolution view of notable changes in urban NOx pollution around the world (2005–2014). J. Geophys. Res.-Atmos. 121 (2):976–996. https://doi.org/10.1002/2015JD024121.
EIA, 2017. US energy information administration, electricity data browser. available at:. https://www.eia.gov/electricity/data/browser/#/topic/0?agg=2,0,1andfuel=vtvvandgeo=vvvvvvvvvvvoandsec=gandfreq=Aandstart=2001andend=2016andctype=linechartandltype=pinandrtype=sandmaptype=0andrse=0andpin, Accessed date: November 2017.
Emami, F., Masiol, M., Hopke, P.K., 2018. Air pollution at Rochester, NY: long-term trends and multivariate analysis of upwind SO2 source impacts. Sci. Total Environ. 612, 1506–1515.
Frampton, M.W., Bausch, J., Chalupa, D., Hopke, P.K., Little, E.L., Oakes, D., Stewart, J.C., Utell, M.J., 2012. Effects of outdoor air pollutants on platelet activation in people with type 2 diabetes. Inhal. Toxicol. 24, 831–838.
Frost, G., McKeen, S., Trainer, M., Ryerson, T., Neuman, J., Roberts, J., Swanson, A., Holloway, J., Sueper, D., Fortin, T., 2006. Effects of changing power plant NO × emissions on ozone in the eastern United States: proof of concept. J. Geophys. Res. 111 (D12):1–19. https://doi.org/10.1029/2005JD006354.
George, C., Ammann, M., D'Anna, B., Donaldson, D.J., Nizkorodov, S.A., 2015. Heterogeneous photochemistry in the atmosphere. Chem. Rev. https://doi.org/10.1021/cr500648z.
HEI Review Panel, 2013. Understanding the Health Effects of Ambient Ultrafine Particles. Health Effect Institute. HEI (Health Effects Institute), Boston, MA, USA.
Hogrefe, C., Lynn, B., Civerolo, K., Ku, J.-Y., Rosenthal, J., Rosenzweig, C., Goldberg, R., Kinney, P., 2004. Simulating changes in regional air pollution over the eastern United States due to changes in global and regional climate and emissions. J. Geophys. Res. D: Atmos. 109 (22):1–13. https://doi.org/10.1029/2004JD004690.
Jeong, C.H., Hopke, P.K., Chalupa, D., Utell, M., 2004. Characteristics of nucleation and growth events of ultrafine particles measured in Rochester, NY. Environ. Sci. Technol. 38 (7):1933–1940. https://doi.org/10.1021/es034811p.
Jeong, C.-H., Evans, G.J., Hopke, P.K., Chalupa, D.J., Utell, M., 2006. Influence of atmospheric dispersion and new particle formation events on ambient particle number concentration in Rochester, United States, and Toronto, Canada. J. Air Waste Manag. Assoc. 56 (4):431–443. https://doi.org/10.1080/10473289.2006.10464519.
Jeong, C.-H., Evans, G.J., McGuire, M.L., Chang, R.Y.-W., Abbatt, J.P.D., Zeromskiene, K., Mozurkewich, M., Li, S.-M., Leaitch, W.R., 2010. Particle formation and growth at five rural and urban sites. Atmos. Chem. Phys. 10 (16):7979–7995. https://doi.org/10.5194/acp-10-7979-2010.
Jeong, C.H., Traub, A., Evans, G.J., 2017. Exposure to ultrafine particles and black carbon in diesel-powered commuter trains. Atmos. Environ. 155:46–52. https://doi.org/10.1016/j.atmosenv.2017.02.015.
Karjalainen, P., Pirjola, L., Heikkila, J., Lahde, T., Tzamkiozis, T., Ntziachristos, L., Keskinen, L., Ronkko, T., 2014. Exhaust particles of modern gasoline vehicles: a laboratory and an on-road study. Atmos. Environ. 97:262–270. https://doi.org/10.1016/j.atmosenv.2014.08.025.
Kasumba, J., Hopke, P.K., Chalupa, D.C., Utell, M.J., 2009. Comparison of sources of submicron particle number concentrations measured at two sites in Rochester, NY. Sci. Total Environ. 407 (18):5071–5084. https://doi.org/10.1016/j.scitotenv.2009.05.040.
Kelly, F.J., Fussell, J.C., 2012. Size, source and chemical composition as determinants of toxicity attributable to ambient particulate matter. Atmos. Environ. 60:504–526. https://doi.org/10.1016/j.atmosenv.2012.06.039.
Kendall, T., 1975. Rank Correlation Methods. 4th ed. Charles Griffin, London, UK.
Kioumourtzoglou, M.A., Schwartz, J.D., Weisskopf, M.G., Melly, S.J., Wang, Y., Dominici, F., Zanobetti, A., 2016. Long-term $PM_{2.5}$ exposure and neurological hospital admissions in the northeastern United States. Environ. Health Perspect. 124 (1):23–29. https://doi.org/10.1289/ehp.1408973.
Knibbs, L.D., Cole-Hunter, T., Morawska, L., 2011. A review of commuter exposure to ultrafine particles and its health effects. Atmos. Environ. 45 (16):2611–2622. https://doi.org/10.1016/j.atmosenv.2011.02.065.
Kulmala, M., Petäjä, T., Ehn, M., Thornton, J., Sipilä, M., Worsnop, D.R., Kerminen, V.-M., 2014. Chemistry of atmospheric nucleation: on the recent advances on precursor characterization and atmospheric cluster composition in connection with atmospheric new particle formation. Annu. Rev. Phys. Chem. 65:21–37. https://doi.org/10.1146/annurev-physchem-040412-110014.
Kumar, P., Pirjola, L., Ketzel, M., Harrison, R.M., 2013. Nanoparticle emissions from 11 non-vehicle exhaust sources - a review. Atmos. Environ. 67:252–277. https://doi.org/10.1016/j.atmosenv.2012.11.011.
Kumar, P., Morawska, L., Birmili, W., Paasonen, P., Hu, M., Kulmala, M., Harrison, R.M., Norford, L., Britter, R., 2014. Ultrafine particles in cities. Environ. Int. 66:1–10. https://doi.org/10.1016/j.envint.2014.01.013.
Lanzinger, S., Schneider, A., Breitner, S., Stafoggia, M., Erzen, I., Dostal, M., et al., 2016. Associations between ultrafine and fine particles and mortality in five central European cities - results from the UFIREG study. Environ. Int. 88:44–52. https://doi.org/10.1016/j.envint.2015.12.006.
Mann, H.B., 1945. Nonparametric tests against trend. Econometrica 13 (3):245–259. https://doi.org/10.1017/CBO9781107415324.004.
Masiol, M., Harrison, R.M., 2014. Aircraft engine exhaust emissions and other airport-related contributions to ambient air pollution: a review. Atmos. Environ. 95:409–455. https://doi.org/10.1016/j.atmosenv.2014.05.070.
Masiol, M., Agostinelli, C., Formenton, G., Tarabotti, E., Pavoni, B., 2014. Thirteen years of air pollution hourly monitoring in a large city: potential sources, trends, cycles and effects of car-free days. Sci. Total Environ. 494–495:84–96. https://doi.org/10.1016/j.scitotenv.2014.06.122.
Masiol, M., Hopke, P.K., Felton, H.D., Frank, B.P., Rattigan, O.V., Wurth, M.J., LaDuke, G.H., 2017a. Analysis of major air pollutants and submicron particles in New York City and Long Island. Atmos. Environ. 148:0–15. https://doi.org/10.1016/j.atmosenv.2016.10.043.
Masiol, M., Hopke, P.K., Felton, H.D., Frank, B.P., Rattigan, O.V., Wurth, M.J., LaDuke, G.H., 2017b. Source apportionment of PM2.5 chemically speciated mass and particle number concentrations in New York City. Atmos. Environ. 148:215–229. https://doi.org/10.5094/APR.2013.018.
May, A.A., Nguyen, N.T., Presto, A.A., Gordon, T.D., Lipsky, E.M., Karve, M., Gutierrez, A., Robertson, W.H., Zhang, M., Brandow, C., Chang, O., Chen, S., Cicero-Fernandez, P., Dinkins, L., Fuentes, M., Huang, S.M., Ling, R., Long, J., Maddox, C., Massetti, J., McCauley, E., Miguel, A., Na, K., Ong, R., Pang, Y., Rieger, P., Sax, T., Truong, T., Vo, T., Chattopadhyay, S., Maldonado, H., Maricq, M.M., Robinson, A.L., 2014. Gas- and particle-phase primary emissions from in-use, on-road gasoline and diesel vehicles. Atmos. Environ. 88:247–260. https://doi.org/10.1016/j.atmosenv.2014.01.046.
McDonald, B.C., Gentner, D.R., Goldstein, A.H., Harley, R.A., 2013. Long-term trends in motor vehicle emissions in US urban areas. Environ. Sci. Technol. 47 (17):10022–10031. https://doi.org/10.1021/es401034z.
Muggeo, V.M.R., 2003. Estimating regression models with unknown break-points. Stat. Med. 22 (19):3055–3071. https://doi.org/10.1002/sim.1545.
Muggeo, V.M.R., 2008. Segmented: an R package to fit regression models with broken-line relationships. R News 8 (May):20–25. https://doi.org/10.1159/000323281.
New York State, 2017. Energy prices, dollars per million Btu: beginning 1970. available at: . https://data.ny.gov/Energy-Environment/Energy-Prices-Dollars-per-Million-Btu-Beginning-19/pzgr-wqm5/data, Accessed date: November 2017.
New York State Compilation of Codes, Rules and Regulations (NYS-CRR), 2017. Chapter III. Air resources, subchapter a. prevention and control of air contamination and air pollution, part 225. Fuel composition and use, subpart 225-1. Fuel composition and use—sulfur limitations. https://govt.westlaw.com/nycrr/Document/I4e971927cd1711dda432a117e6e0f345?viewType=FullTextandoriginationContext=documenttocandtransitionType=CategoryPageItemandcontextData=(sc.Default)andbhcp=1.
Nopmongcol, U., Jung, J., Kumar, N., Yarwood, G., 2016. Changes in US background ozone due to global anthropogenic emissions from 1970 to 2020. Atmos. Environ. 140:446–455. https://doi.org/10.1016/j.atmosenv.2016.06.026.
O'Dowd, C., Monahan, C., Dall'Osto, M., 2010. On the occurrence of open ocean particle production and growth events. Geophys. Res. Lett. 37 (19):2–6. https://doi.org/10.1029/2010GL044679.
Ogulei, D., Hopke, P.K., Chalupa, D.C., Utell, M.J., 2007. Modeling source contributions to submicron particle number concentrations measured in Rochester, New York. Aerosol Sci. Technol. 41 (2):179–201. https://doi.org/10.1080/02786820601116012.
Ostro, B., Hu, J., Goldberg, D., Reynolds, P., Hertz, A., Bernstein, L., Kleeman, M.J., 2015. Associations of mortality with long-term exposures to fine and ultrafine particles, species and sources: results from the California teachers study cohort. Environ. Health Perspect. 123 (6):549–556. https://doi.org/10.1289/ehp.1408565.
Pant, P., Harrison, R.M., 2013. Estimation of the contribution of road traffic emissions to particulate matter concentrations from field measurements: a review. Atmos. Environ. 77:78–97. https://doi.org/10.1016/j.atmosenv.2013.04.028 (Review).
Pye, H.O.T., Liao, H., Wu, S., Mickley, L.J., Jacob, D.J., Henze, D.J., Seinfeld, J.H., 2009. Effect of changes in climate and emissions on future sulfate-nitrate-ammonium aerosol levels

in the United States. J. Geophys. Res.-Atmos. 114 (1). https://doi.org/10.1029/2008JD010701.
Qian, S., Sakurai, H., McMurry, P.H., 2007. Characteristics of regional nucleation events in urban East St. Louis. Atmos. Environ. 41 (19):4119–4127. https://doi.org/10.1016/j.atmosenv.2007.01.011.
R Core Team, 2017. A Language and Environment for Statistical Computing. R Foundation for Statistical Computing.
Reche, C., Viana, M., Moreno, T., Querol, X., Alastuey, A., Pey, J., Pandolfi, M., Prévôt, A., Mohr, C., Richard, A., Artiñanod, B., Gomez-Morenod, J., Cots, N., 2011. Peculiarities in atmospheric particle number and size-resolved speciation in an urban area in the western Mediterranean: results from the DAURE campaign. Atmos. Environ. 45 (30):5282–5293. https://doi.org/10.1016/j.atmosenv.2011.06.059.
Rich, D.Q., Zareba, W., Beckett, W., Hopke, P.K., Oakes, D., Frampton, M.W., Bisognano, J., Chalupa, D., Bausch, J., O'Shea, K., Wang, Y., Utell, M.J., 2012. Are ambient ultrafine, accumulation mode, and fine particles associated with adverse cardiac responses in patients undergoing cardiac rehabilitation? Environ. Health Perspect. 120, 1162–1169.
Rich, D.Q., Peters, A., Schneider, A., Zareba, W., Breitner, S., Oakes, D., Wiltshire, J., Kane, C., Frampton, M.W., Hampel, R., Hopke, P.K., Cyrys, J., Utell, M.J., 2016. Ambient and controlled particle exposures as triggers for acute ECG changes. Res. Rep. Health Eff. Inst. 186, 5–75.
Riffault, V., Arndt, J., Marris, H., Mbengue, S., Setyan, A., Alleman, L.Y., Deboudt, K., Flament, P., Augustin, P., Delbarre, H., 2015. Fine and ultrafine particles in the vicinity of industrial activities: a review. Crit. Rev. Environ. Sci. Technol. 45 (21):2305–2356. https://doi.org/10.1080/10643389.2015.1025636.
Rohr, A.C., Wyzga, R.E., 2012. Attributing health effects to individual particulate matter constituents. Atmos. Environ. 62:130–152. https://doi.org/10.1016/j.atmosenv.2012.07.036.
Rose, C., Sellegri, K., Velarde, F., Moreno, I., Ramonet, M., Weinhold, K., Krejci, R., Andrade, M., Wiedensohler, A., Laj, P., 2015. Frequent nucleation events at the high altitude station of Chacaltaya (5240 m a.s.l.), Bolivia. Atmos. Environ. 102:18–29. https://doi.org/10.1016/j.atmosenv.2014.11.015.
Sabaliauskas, K., Jeong, C.H., Yao, X., Jun, Y.-S., Jadadian, P., Evans, G.J., 2012. Five-year roadside measurements of ultrafine particles in a major Canadian city. Atmos. Environ. 49:245–256. https://doi.org/10.1016/j.atmosenv.2011.11.052.
Salma, I., Füri, P., Németh, Z., Balásházy, I., Hofmann, W., Farkas, A., 2015. Lung burden and deposition distribution of inhaled atmospheric urban ultrafine particles as the first step in their health risk assessment. Atmos. Environ. 104:39–49. https://doi.org/10.1016/j.atmosenv.2014.12.060.
Salma, I., Németh, Z., Kerminen, V.-M., Aalto, P., Nieminen, T., Weidinger, T., Molnár, Á., Imre, K., Kulmala, M., 2016. Regional effect on urban atmospheric nucleation. Atmos. Chem. Phys. 16 (14):8715–8728. https://doi.org/10.5194/acp-16-8715-2016.
Seinfeld, J.H., Pandis, S.N., 2016. Atmospheric chemistry and physics: from air pollution to climate change. Atmospheric Chemistry and Physics, 3rd ed. John Wiley and Sons, New York, NY, USA https://doi.org/10.1080/00139157.1999.10544295.
Sen, P.K., 1968. Estimates of the regression coefficient based on Kendall's Tau. J. Am. Stat. Assoc. 63 (324):1379–1389. https://doi.org/10.2307/2285891.
Shi, L., Zanobetti, A., Kloog, I., Coull, B.A., Koutrakis, P., Melly, S.J., Schwartz, J.D., 2016. Low-concentration $PM_{2.5}$ and mortality: estimating acute and chronic effects in a population-based study. Environ. Health Perspect. 124 (1):46–52. https://doi.org/10.1289/ehp.1409111.
Stanier, C.O., Khlystov, A.Y., Pandis, S.N., 2004. Nucleation events during the Pittsburgh air quality study: description and relation to key meteorological, gas phase, and aerosol parameters special issue of aerosol science and technology on findings from the fine particulate matter supersites program. Aerosol Sci. Technol. 38 (March):253–264. https://doi.org/10.1080/02786820390229570.
Strak, M., Janssen, N.A., Godri, K.J., Gosens, I., Mudway, I.S., Cassee, F.R., Lebret, E., Kelly, F.J., Harrison, R.M., Brunekreef, B., Steenhof, M., Hoek, G., 2012. Respiratory health effects of airborne particulate matter: the role of particle size, composition, and oxidative potential-the RAPTES project. Environ. Health Perspect. 120 (8):1183–1189. https://doi.org/10.1289/ehp.1104389.
Tagaris, E., Manomaiphiboon, K., Liao, K.J., Leung, L.R., Woo, J.H., He, S., ... Russell, A.G., 2007. Impacts of global climate change and emissions on regional ozone and fine particulate matter concentrations over the United States. J. Geophys. Res.-Atmos. 112 (14). https://doi.org/10.1029/2006JD008262.
Theil, H., 1950. A rank-invariant method of linear and polynomial regression analysis. Proceedings of the royal Netherlands. Acad. Sci. 53:386–392. https://doi.org/10.1007/978-94-011-2546-8_20.
U.S. Environmental Protection Agency (US EPA), 2016a. Heavy-Duty Highway Compression-Ignition Engines and Urban Buses: Exhaust Emission Standards, Office of Transportation and Air Quality, EPA-420-B-16-018. March 2016. https://nepis.epa.gov/Exe/ZyPDF.cgi?Dockey=P100O9ZZ.pdf.
U.S. Environmental Protection Agency (US EPA), 2016b. Highway and Nonroad, Locomotive, and Marine (NRLM) Diesel Fuel Sulfur Standards, Office of Transportation and Air Quality, EPA-420-B-16-005. March 2016. https://nepis.epa.gov/Exe/ZyPDF.cgi?Dockey=P100O9ZI.pdf.
U.S. Environmental Protection Agency (US EPA), 2017. Light-duty Vehicles, Light-duty Trucks, and Medium-duty Passenger Vehicles: Tier 2 Exhaust Emission Standards and Implementation, Office of Transportation and Air Quality, EPA-420-B-17-028 September 2017 Schedule. https://nepis.epa.gov/Exe/ZyPDF.cgi/P100SMQA.PDF?Dockey=P100SMQA.PDF.
Valavanidis, A., Fiotakis, K., Vlachogianni, T., 2008. Airborne particulate matter and human health: toxicological assessment and importance of size and composition of particles for oxidative damage and carcinogenic mechanisms. Journal of Environmental Science and Health, Part C 26 (4):339–362. https://doi.org/10.1080/10590500802494538.
Wang, Y., Hopke, P.K., Chalupa, D.C., Utell, M.J., 2011a. Long-term study of urban ultrafine particles and other pollutants. Atmos. Environ. 45 (40):7672–7680. https://doi.org/10.1016/j.atmosenv.2010.08.022.
Wang, Y., Hopke, P.K., Chalupa, D.C., Utell, M.J., 2011b. Effect of the shutdown of a coal-fired power plant on urban ultrafine particles and other pollutants. Aerosol Sci. Technol. 45:1245–1249. https://doi.org/10.1080/02786826.2011.588730.
Wang, Y., Hopke, P.K., Utell, M.J., 2012. Urban-scale seasonal and spatial variability of ultrafine particle number concentrations. Water Air Soil Pollut. 223 (5):2223–2235. https://doi.org/10.1007/s11270-011-1018-z.
Wang, J., Xing, J., Mathur, R., Pleim, J.E., Wang, S., Hogrefe, C., Gan, C.M., Wong, D.C., Hao, J., 2017. Historical trends in $PM_{2.5}$-related premature mortality during 1990–2010 across the Northern Hemisphere. Environ. Health Perspect. 125 (3):400–408. https://doi.org/10.1289/EHP298.
Wood, S.N., 2001. Minimizing model fitting objectives that contain spurious local minima by bootstrap restarting. Biometrics 57 (1):240–244. https://doi.org/10.1111/j.0006-341X.2001.00240.x.
Yu, F., Luo, G., Bates, T., Anderson, B., Clarke, A., Kapusin, V., Yantosca, R., Wang, Y., Wu, S., 2010. Spatial distributions of particle number concentrations in the global troposphere: simulations, observations, and implications for nucleation mechanisms. J. Geophys. Res.-Atmos. 115 (17):1–14. https://doi.org/10.1029/2009JD013473.
Yu, F., Luo, G., Pryor, S.C., Pillai, P.R., Lee, S.H., Ortega, J., Schwab, J.J., Hallar, A.G., Leaitch, W. R., Aneja, V.P., Smith, J.N., Walker, J.T., Hogrefe, O., Demerjian, K.L., 2015. Spring and summer contrast in new particle formation over nine forest areas in North America. Atmos. Chem. Phys. 15 (24):13993–14003. https://doi.org/10.5194/acp-15-13993-2015.
Zeileis, A., Grothendieck, G., 2005. zoo: S3 infrastructure for regular and irregular time series. J. Stat. Softw. 14 (6):1–27. https://doi.org/10.18637/jss.v014.i06.
Zhang, R., Khalizov, A., Wang, L., Hu, M., Xu, W., 2012. Nucleation and growth of nanoparticles in the atmosphere. Chem. Rev. 112, 1957–2011.